

# Evidence for excitonic behavior of photoluminescence in polymer-like a-C:H films

C. Godet<sup>a,\*</sup>, M.N. Berberan-Santos<sup>b</sup>

<sup>a</sup>Laboratoire PICM (CNRS-UMR 7647) Ecole Polytechnique, 91128 Palaiseau-Cedex, France

<sup>b</sup>Centro de Química-Física Molecular, Instituto Superior Técnico, Av. Rovisco Pais, Lisboa 1049-001, Portugal

## Abstract

To understand the dynamics of energy transfer and randomization of photoluminescence polarization in hydrogen-rich polymer-like amorphous carbon a-C:H films, time-resolved investigations of intensity and anisotropy decays have been performed recently. The intensity decay rates increase exponentially as a function of emission energy with a behavior very similar to that observed in wide band-gap C-rich a-Si<sub>1-x</sub>C<sub>x</sub>:H. In addition, in polymer-like carbon, the observation of a plateau of PL anisotropy in the 100–1000 ps range, is taken as strong evidence for the existence of a finite density of excitonic species in radiative recombination phenomena; it does not fit the phonon-assisted depolarization models proposed earlier. Polarization anisotropy decays and steady-state values are consistently interpreted using a dipole–dipole non-radiative energy transfer mechanism (Förster mechanism) with a characteristic depolarization time of 50 ps rather independent of the emission energy. The latter value is likely to be related to the density of radiative centers distribution estimated independently in the constant exciton radius approximation, rather than the result of hopping in an exponential distribution of tail states. © 2001 Elsevier Science B.V. All rights reserved.

**Keywords:** Amorphous carbon; Luminescence; Exciton; Polarization spectroscopy

## 1. Introduction

As a consequence of the allotropic properties of carbon, both nanostructure and optoelectronic properties of carbon-based films are strongly dependent on the deposition conditions. Hydrogen incorporation introduces additional degrees of freedom into the atomic structure, leading to low density carbon films. The  $\pi$ -bonding favors a segregation between  $sp^2$  and  $sp^3$  sites, so that  $sp^2$  sites can pair up to form chain or ring configurations. This medium range organization related to conjugation of  $\pi$ -bonds confers a high versatility to optical and transport properties of carbon thin-films [1].

Hydrogenated amorphous carbon (a-C:H) films are also potentially interesting for the deposition of large area electronic devices at low temperatures, compatible with polymer substrates. However, so far, the development of light emitting diodes [2], heterojunction photovoltaic devices [3], thin-film transistors [4] and field emission devices [5] remains far from expectations. The achievement of a good quality electronic material cannot be separated from a detailed understanding of the relationship between growth mechanisms, film nanostructure and the resulting electronic density of states (DOS).

In amorphous carbon films containing both  $sp^2$ - and  $sp^3$ -hybridized C atoms, the weaker  $\pi$ -bonding and the orientation dependence of the  $\pi$  interaction cause the localization of the entire  $\pi$ - and  $\pi^*$ -bands within the  $\sigma$ - $\sigma^*$ -gap [6]. Strong site-to-site potential fluctuations result from the large difference between  $\pi$ - and  $\sigma$ -bond

\* Corresponding author. Tel.: +33-1-69-33-32-10; fax: +33-1-69-33-30-06.

E-mail address: godet@poly.polytechnique.fr (C. Godet).

energies, which in turn lead to low carrier hopping mobilities [4,7] and, in some cases, strong luminescence efficiency.

In polymer-like a-C:H films, characterized by high H content, low C atom density, low dielectric constant and wide band-gap, the strong confinement of photo-generated electron-hole pairs inside  $\pi$ -bonded ‘grains’ is supported experimentally by the intense PL in the visible spectrum at the ambient temperature. The lower PL efficiency observed for denser a-C:H films has been tentatively explained by a decrease of the pair confinement due to stress-induced  $\sigma$ - $\pi$  orbital mixing [8].

Further indications of strong confinement have been reported such as: (i) the lack of thermal quenching of PL intensity [9]; (ii) the anisotropy (polarization memory) of photoluminescence obtained using linearly polarized excitation light [10–12]; (iii) the fast (sub-nanosecond) decay of PL intensity [12,13]; and (iv) the constant decay time as a function of generation rate [13].

As far as intensity decay rates are concerned, they are found to increase exponentially as a function of emission energy over a broad spectral range. Interestingly, this behavior is found to be very similar for different types of carbon-based thin-films with wide band-gap ( $E_{04} \approx 4.0$  eV) such as ECR-grown C-rich a-Si<sub>1-x</sub>C<sub>x</sub>:H [14] and dual-plasma (r.f.-assisted microwave plasma) a-C:H [12]. This common behavior shown in Fig. 1 might indicate an intrinsic property of  $\pi$ -bonded materials but it has also been found in silicon nitride insulating films and multilayers [15]. It has been suggested that non-radiative (NR) lifetimes govern the experimental decay times, through the dissociation of excitonic electron-hole pairs mediated by the electron tunneling towards a vacant site at the same energy [8].

In a recent report [12], anisotropy decays and steady-state values have been consistently interpreted

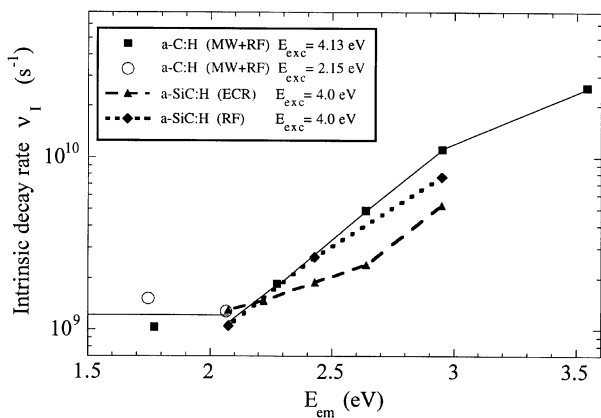


Fig. 1. Emission energy dependence of PL intensity decay rates using pulsed laser excitation for wide band-gap a-C:H [12] and a-Si<sub>x</sub>C<sub>1-x</sub>:H films [14].

using a dipole–dipole non-radiative energy transfer mechanism (Förster mechanism [16,17] with a characteristic depolarization time of 50 ps). For emission energies  $E_{em}$  between 1.8 and 3.5 eV, anisotropy decreases within 100 ps and reaches a plateau within 1 ns. This observation has been explained by the transfer of electronic excitation towards a finite density of luminescent centers but it is not consistent with previous models based on phonon-assisted depolarization [10,18] which should occur on a much shorter (sub-picosecond) time scale. However, in this paper, we will first consider the role of thermalization of photoexcitation in disordered insulators in the frame of the ‘trapped exciton’ model proposed by Kivelson and Gelatt [19].

In the second part, we will analyze in more detail the photoluminescence intensity and anisotropy decays in the picosecond–nanosecond range reported recently [12] for polymer-like a-C:H, excited using a linearly polarized UV photon beam. The polarization spectroscopy results will be discussed in terms of exciton-like radiative recombination and the characteristic depolarization time constant of 50 ps (nearly constant for emission energies in the range 1.5–3.5 eV) will be related to the density of radiative centers, estimated by two independent methods: (a) the Förster intensity decay for primarily excited chromophores, and (b) the spectral density method using a constant exciton radius approximation.

## 2. Energy relaxation

In this section, we consider thermalization mechanisms which occur before and during radiative recombination. In particular, we address the dynamics of the hopping motion of either a single charged carrier or a neutral exciton through a band of localized states and we discuss their respective relaxation rates.

A number of photoluminescence investigations of polymer-like carbon films, including excitation spectra and polarization memory properties, indicate that radiative recombination arises from exciton-like electron-hole pairs with a strong Coulomb interaction [8]. In the trapped exciton model [19] proposed earlier to describe spectroscopic and dynamic properties of photoluminescence in disordered insulators, one of the carriers is trapped in a highly localized state in the pseudogap and the other carrier is bound to the first by their mutual Coulomb attraction in a large ‘hydrogenic’ state.

In the hydrogenoid model of excitons applied to polymer-like carbon [8], typical values of the exciton radius  $a_B^* = (4\pi\epsilon_0\epsilon\hbar^2)/\mu^*e^2 \approx 6$  Å and binding energy  $E_B = e^2/8\pi\epsilon_0\epsilon a_B^* \approx 0.40$  eV, have been estimated (using a dielectric constant  $\epsilon = 3$  and the analog of a reduced mass  $\mu^* \approx m_e^* \approx 0.25 m_e$ ).

As developed in the next section, the fact that the anisotropy conferred by a polarized photon beam excitation is retained partially by thermalized electron-hole pairs which recombine radiatively is explained by a Coulomb attraction stronger than local potential fluctuations seen by photogenerated electron-hole pairs during their thermalization.

According to the trapped exciton theory for amorphous systems [19], a fraction of the photo-generated electron hole-pairs may dissociate (giving 2 single carriers at a distance beyond the Coulomb interaction radius) before the formation of an excitonic pair occurs. The efficiency of exciton formation is expected to depend mainly on the excess energy provided by the exciting photon. However, experimental results reported by Kóos et al. [20] indicate that the PL efficiency is not affected at least up to approximately 5 eV excitation energy. This can be explained by the very low hopping mobility of carriers in the localized states arising from the  $\pi$ -bonded carbon matrix [4,7] and the very high energy barrier to access extended  $\sigma$  states [6].

After optical excitation, exciton thermalization occurs by a phonon-assisted hopping mechanism which is mainly related to the hole thermalization, due to the band tail asymmetry [19]. Hence, the dynamics of hole thermalization dominates the luminescence spectrum, i.e. the distribution of total exciton energies is largely determined by the spread in hole energies.

Alternative descriptions of photoluminescence in carbon films [21] are inspired by the PL properties of a-Si:H films [22,23] where weaker Coulomb interactions prevail owing to the higher dielectric constant. In the submicrosecond range however, low temperature PL in a-Si:H is consistent with exciton formation [24]. In the weak Coulomb interaction case, in the picosecond–nanosecond time-scale following photo-generation, the photogenerated electron and hole (with initially overlapping wavefunctions) are assumed to thermalize separately by hopping apart in their respective band tails.

In summary, energy relaxation of carriers excited in a distribution of localized states is likely to occur by energy-loss hopping, either as single carriers in their respective tail states or as excitons made of carrier pairs bound by their mutual Coulomb attraction. In the following, we derive some specific features expected for each type of hopping mechanism.

Energy relaxation by hopping in a distribution of localized states, randomly distributed in a three-dimensional homogeneous space, is considered. This model applies to amorphous carbon and carbon alloys where bonding and antibonding  $\pi$  orbitals produce highly localized states decoupled from extended  $\sigma$ -states [6].

An exponential energy-dependence of the density-of-states (DOS) distribution is assumed:

$$N(E) = (N_0/E^\circ)\exp(E/E^\circ). \quad (1)$$

We consider here a low-temperature regime where excited species can only hop to sites of lower energy. Hence the density of available sites for a carrier at energy  $E_1$  is:

$$N_{av}(E_1) = N_0\exp(E_1/E^\circ). \quad (2)$$

The rate of direct tunneling for a single carrier hopping from occupied site ( $i$ ) to unoccupied site ( $j$ ) is given by:

$$\Gamma_{ij} = \nu_0\exp(-2\gamma R_{ij}) \quad E_i \geq E_j \quad (3)$$

where the attempt-to-escape frequency  $\nu_0$  is considered to be independent on  $E_i$  and  $E_j$  and  $(1/\gamma)$  is a carrier localization radius. The time-dependent mean energy of the excited carrier population is given by:

$$E_C(t) = -2E^\circ\ln(\ln(\nu_0 t)) \quad (4)$$

corresponding to a relaxation rate decreasing as a function of time:

$$\partial E_C/\partial \ln(t) = -3E^\circ/\ln(\nu_0 t) \quad (5)$$

For composite particles such as excitons, hopping may be mediated by a dipole–dipole interaction (Förster mechanism [16,17]) which takes place when the spectral density of a donor site ( $i$ ) overlaps the absorption spectrum of an acceptor site ( $j$ ). As developed in the next section, the interaction strength is a power function of the distance:

$$\Gamma_{ij} = \Gamma_E(R_0/R_{ij})^6 \quad (6)$$

For large hopping lengths, the latter hopping mechanism is expected to dominate. The time-dependent mean energy of the excited carrier population is given by:

$$E_E(t) = -(E^\circ/2)\ln((4\pi/3)^2 R_0^6 N_0^2 \Gamma_E t) \quad (7)$$

corresponding to a constant relaxation rate:

$$\partial E_E/\partial \ln(t) = -E^\circ/2 \quad (8)$$

As a consequence of the strongly different dependences of hopping rates on hopping lengths, the faster thermalization is expected for single carrier relaxation at short times and for exciton relaxation at longer times. In a first approximation, we use the same  $E^\circ$  values for single carriers and excitons, corresponding to the broader of the valence and conduction band-tails [19]. Using Eq. (5) and Eq. (8) and setting the attempt-

to-escape frequency as a phonon frequency  $\nu_0 = 1 \times 10^{13} \text{ s}^{-1}$ , a cross-over between both regimes is expected for a typical time scale  $\tau^* \approx 40 \text{ ps}$ . The coincidence with the PL depolarization time in a-C:H is probably fortuitous.

It is stressed that both hopping processes contribute to the non-polarized part of photoluminescence emission. In a polarization spectroscopy experiment, the single carriers have lost the memory of the linearly polarized excitation during the first 0.1–1-picosecond (thermalization by phonon emission) while the excitonic pairs are characterized by a depolarization frequency  $\nu_{\text{DP}}$  which reflects the strength of dipole–dipole energy transfer, as explained in the next section.

### 3. Polarization spectroscopy

Polarization spectroscopy is a powerful experimental tool for investigating structural and kinetic properties of complex molecular systems. In any system, whether anisotropic or isotropic, the absorption of photons from a polarized beam confers a degree of anisotropy, which persists until it is lost through molecular motion or energy randomization. Typical time scales depend on the randomization process itself, ranging from  $10^{-14}$ – $10^{-12} \text{ s}$  for carrier thermalization (phonon exchange),  $10^{-11}$ – $10^{-8} \text{ s}$  for non-radiative energy transfer,  $10^{-9}$ – $10^{-1} \text{ s}$  for (allowed vs. forbidden) radiative processes and  $10^{-6}$ – $10^{+4} \text{ s}$  for viscous flow (molecular motion). Over a timescale determined by some of these dynamical effects, a complex system excited by photon absorption can reveal its conferred transient anisotropy through secondary optical processes such as luminescence.

Experimental evidence for exciton motion in insulating solids is firmly established [17]. The technique most often used to measure the diffusion coefficient of excitons has been that of sensitized fluorescence, which refers to the fluorescence of a guest indicator species, usually present in low concentrations in the host matrix; this emission is not due to the direct excitation of the guest by light but rather is due to the transfer of excitation energy from the host, which acts as the antenna (Fig. 2). In polymer-like carbon films, a continuous manifold of localized  $\pi$  states is expected, corresponding to the radiative centers (chromophores) which may act as both donors or acceptors of electronic excitation, depending on the energetics. The exciton then moves incoherently and generally is viewed as a localized excitation undergoing a random hopping-like motion between  $\pi$  states.

A possible depolarization mechanism often reported in polymers is radiationless excitation transfer from a donor to an acceptor chromophore via incoherent resonant dipole–dipole interactions (Förster mechanism)

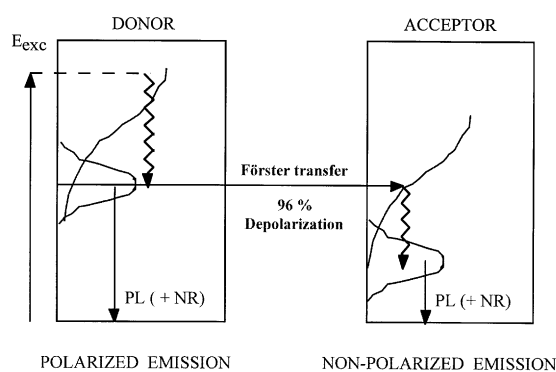


Fig. 2. Principle of the non-radiative dipole–dipole energy transfer (Förster mechanism) where the PL spectral density distribution of the donor site overlaps the absorption spectrum of the acceptor site. In disordered materials, broad optical absorption edges and Gaussian-like PL spectral densities are expected. Wavy arrows indicate thermalization of electronic excitation.

[16,17]. For each transfer the depolarization efficiency is at least 96% in a random medium. In this electric dipole mediated interaction, the excitation transfer rate ( $\nu$ ) is proportional to the energy overlap between the emission spectral density of donor sites and the absorption spectrum of acceptor sites, separated by a distance  $R$ , and can be expressed as:

$$\nu = (1/\tau_I)(R_0/R)^6 \quad (9)$$

where  $\tau_I$  is the intrinsic (radiative and non-radiative) decay time and the effective critical Förster radii  $R_0$  (which defines equal probabilities for decay or transfer) usually take values between 20 and 60 Å [16]. Hence, for excitons located at primarily excited (polarized) chromophores, with a characteristic depolarization time of 50 ps (Fig. 3), typical exciton diffusion coefficients are on the order of  $D_{\text{exc}} \approx 8 \times 10^{-4}$ – $7 \times 10^{-3} \text{ cm}^2 \text{ s}^{-1}$ .

In our interpretation of time-resolved PL, we assume that pair dissociation or radiative recombination only

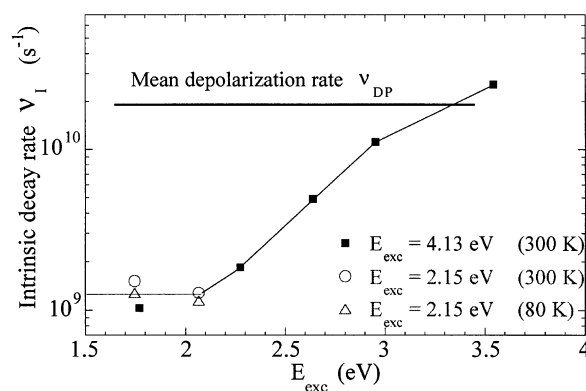


Fig. 3. Intensity decay rates  $\nu_1(E_{\text{em}})$  obtained from time-resolved decays fitted using a sum of 3 exponentials. The horizontal line is an average of depolarization rate values obtained at 5 different energies between 1.7 and 3.5 eV [12].

occurs after a fast thermalization of the exciton-like pair corresponding to relaxation of the excess energy by phonon emission within typically 1 ps. If the thermalized exciton is in thermal equilibrium with its surroundings, the dynamic characteristics of PL should be excitation energy independent. This is indeed observed in Fig. 3 for emission at  $E_{em} = 1.75$  eV excited using either  $E_{exc} = 2.15$  eV or  $E_{exc} = 4.13$  eV.

#### 4. Energy distribution of radiative centers

Polarization anisotropy decays and steady-state values have been consistently interpreted using a dipole–dipole non-radiative energy transfer mechanism (Förster mechanism) leading to characteristic depolarization times (50 ps) rather independent of the emission energy. In order to understand the latter values, we estimate the density distribution of the radiative centers, using two independent methods: (a) the Förster intensity decay for primarily excited chromophores; and (b) the spectral density method using a constant exciton radius approximation.

##### 4.1. Förster intensity decay

It is stressed that the Förster decay equation strictly applies to emission close to the excitation energy, corresponding to primarily excited chromophores, in contrast with emission at energies much lower than the excitation energy, which include a significant number of acceptors. Assuming a random distribution of chromophores, the decay law of initially excited donors is known to be given by:  $i(t) = \exp[-(t/\tau_F) - b t^{1/2}]$  where  $b$  ( $\text{ps}^{-1/2}$ ) =  $0.845 n_A [\pi/\tau_F]^{1/2}$  and  $n_A = 4/3$

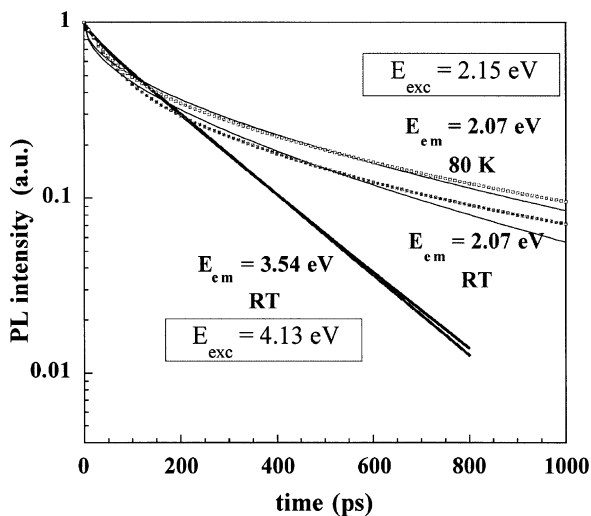


Fig. 4. PL intensity decays at  $E_{em} = 3.54$  eV using  $E_{exc} = 4.13$  eV (at 300 K), at  $E_{em} = 2.07$  eV using  $E_{exc} = 2.15$  eV (at 80 and 300 K) with the fitted Förster decay superimposed to experimental data.

$\pi N_A [R_0]^3$  is a number of acceptor molecules within a sphere of radius  $R_0$ .

A fit of this equation to the PL intensity decays at 3.54 and 2.07 eV (Fig. 4) yields the following values for  $n_A$  (3.54 eV) = 0.16 and  $n_A$  (2.07 eV) = 1.7 corresponding to densities of acceptor molecules:  $N_A$  (3.54 eV)  $\approx 2.0 \times 10^{17} - 5.5 \times 10^{18} \text{ cm}^{-3}$ ; and  $N_A$  (2.07 eV)  $\approx 2.2 \times 10^{18} - 5.9 \times 10^{19} \text{ cm}^{-3}$  (for typical values of the Förster radii  $R_0$  between 20 and 60 Å).

Surprisingly, one order of magnitude higher values are obtained for the density of acceptors at lower emission energies. This result does not fit the usual picture of an exponential distribution of localized states, vanishing at low energies. Coherence can be partially restored if one assumes that the spatial distribution of the low energy species is not random (as assumed by the model) but rather clustered, having therefore, an effective local concentration higher than expected. This would not affect the decay behavior for high energies, where the acceptors (still at higher energies than these entities) could still be assumed to be randomly distributed.

On the other hand, since the ‘effective’ Förster radius  $\langle R_0 \rangle$  depends on the 1/6th power of the PL yield [17] a larger  $\langle R_0 \rangle$  and hence smaller  $N_A$  than calculated, are expected at lower emission energies.

##### 4.2. Density of excitonic radiative centers

In order to check for the latter model-dependent result, the effective density of radiative excitonic centers  $N_E(E_{em})$  can be obtained independently from the PL spectral density  $W(E_{em})$ , using:

$$W(E_{em}) = (\nu_{rad}/\nu_I) N_E(E_{em}) \quad (10)$$

provided the radiative decay rate  $\nu_{rad}$  and the intensity decay rate  $\nu_I$  are known as a function of emission energy  $E_{em}$ . The latter has been measured for several

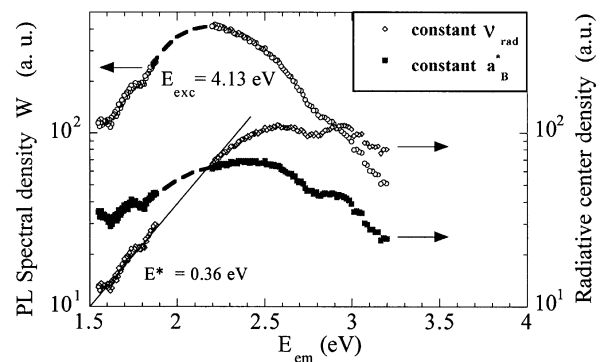


Fig. 5. Spectral density  $W(E_{em})$  of PL using unpolarized excitation at  $E_{exc} = 4.13$  eV. The density of radiative centers has been obtained in two different approximations: (a)  $E_{em}$ -independent radiative rate  $\nu_{rad}$ , and (b)  $E_{em}$ -independent exciton radius  $a_B^*$ .

energies in the range 1.7–3.5 eV [12] and can be interpolated as shown in Fig. 3. If one assumes a constant radiative rate, one obtains for the radiative center distribution an exponential edge at lower energies with characteristic slope  $E^* \approx 0.36$  eV, followed by a plateau at higher energy (Fig. 5). However, this situation is not physical because two energy-dependent terms should be considered.

The emission energy dependence of the exciton radiative decay rate is difficult to measure or to assess on theoretical grounds, since an exact expression of the confined electron and hole wavefunctions would be very complex. We can only derive basic tendencies for the radiative recombination rate as a function of exciton localization. Although olefinic chains or aromatic rings are strongly anisotropic, we assume that a spherical approximation holds with a radial decay given by an effective electron Bohr radius. The radius of the hole state ( $a_H$ ) and the exciton radius ( $a_{B1}^*$ ) determine the radiative recombination rate. The radiative transition is described as a dipolar electric transition of an electron from an initial state to an unoccupied final state separated by an energy  $E_{cm}$ . The radiative transition rate:

$$\nu_{rad} = Cte \varepsilon^{1/2} E_{cm}^3 (a_B^* a_H^*)^5 / (a_B^* + a_H^*)^8 \quad (11)$$

is approximated by  $\nu_{rad} \approx \varepsilon^{1/2} E_{cm}^3 a^5 / (a_B^*)^3$  if the hole radius is close to one interatomic distance ( $a$ ) with:  $(a) \ll (a_B^*)$ .

On the basis of a constant exciton radius ( $a_B^*$ ), and taking into account the factor ( $E_{cm}^3$ ), one finds a broad (FWHM  $\approx 0.85$  eV) distribution of excitonic states rather symmetrical and centered near 2.35 eV. Such a broad distribution is expected due to the effects of the local environments on the radiative centers. However, this result does not take into account the possible dependence of the radiative rates as a function of exciton confinement ( $a_B^*$ ). In this constant exciton radius approximation, the results shown in Fig. 5 are qualitatively consistent with the PL intensity decays modeled by the Förster equation.

## 5. Conclusion

PL characteristics of polymer-like carbon films indicate that excitonic species are efficiently photo-generated using visible and UV excitation energies. This polarization spectroscopy study indicates that excitonic luminescent centers have a broad energy distribution, as obtained by two independent methods, which does not follow the overall distribution of  $\pi$  and  $\pi^*$  states, as measured by optical absorption techniques [25].

However, the latter sites are available for exciton dissociation by electron tunneling, which may eventually lead to non-radiative recombination. The existence of a broad distribution of radiative centers is consistent with the quasi-energy independent depolarization rate of  $2 \times 10^{10} \text{ s}^{-1}$ .

## Acknowledgements

The authors wish to thank T. Heitz, J.E. Bourée (Ecole Polytechnique, Palaiseau), J.P. Conde and A. Fedorov (IST, Lisbon) for stimulating discussions and participation in the experimental characterizations of carbon films.

## References

- [1] J. Robertson, *Adv. Phys.* 35 (1986) 317.
- [2] M. Yoshimi, H. Shimizu, K. Hattori, H. Okamoto, Y. Hamakawa, *Optoelectronics* 7 (1992) 69.
- [3] K.M. Krishna, Y. Nukaya, T. Soga, T. Jimbo, M. Umeno, *Solar Energy Mat. Solar Cells* 65 (2001) 163.
- [4] F.J. Clough, W.I. Milne, B. Kleinsorge, J. Robertson, G.A.J. Amarutunga, B.N. Roy, *Electron. Lett.* 32 (1996) 498.
- [5] J. Robertson, *Mater. Res. Soc. Symp. Proc.* 621 (2000).
- [6] C.W. Chen, J. Robertson, *J. Non-Cryst. Solids* 227 (1998) 602.
- [7] C. Godet, *Phil. Mag. B*, 2000, to be published.
- [8] T. Heitz, C. Godet, J.E. Bourée, B. Drévilon, J.P. Conde, *Phys. Rev. B* 60 (1999) 6045.
- [9] S.V. Chernyshov, E.I. Terukov, V. Vassilyev, A.S. Volkov, *J. Non-Cryst. Solids* 134 (1991) 218.
- [10] M. Koos, I. Pocsik, L. Toth, *J. Non-Cryst. Solids* 164–166 (1993) 1151.
- [11] Rusli, G.A.J. Amarutunga, J. Robertson, *Phys. Rev. B* 53 (1996) 16306.
- [12] M.N. Berberan-Santos, A. Fedorov, J.P. Conde, C. Godet, T. Heitz, J.E. Bourée, *Chem. Phys. Lett.* 319 (2000) 113.
- [13] W. Lormes, M. Hundhausen, L. Ley, *J. Non-Cryst. Solids* 227–230 (1998) 570.
- [14] J.P. Conde et al., *J. Appl. Phys.* 85 (1999) 3327.
- [15] F. Giorgis, C.F. Pirri, C. Vinegoni, L. Pavesi, *J. Lumin.* 80 (1999) 423.
- [16] M.D. Galanin, *Luminescence of Molecules and Crystals*, Cambridge International Science Publishing, Cambridge, 1996.
- [17] M. Pope, C.E. Swenberg, *Electronic Processes in Organic Crystals*, Clarendon Press, Oxford, 1982.
- [18] Y. Masumoto, H. Kunitomo, S. Shionoya, H. Munekata, H. Kukimoto, *Solid State Commun.* 51 (1984) 209.
- [19] S. Kivelson, C.D. Gelatt, *Phys. Rev. B* 26 (1982) 4646.
- [20] M. Koos, I. Pocsik, J. Erostyak, A. Buzady, *J. Non-Cryst. Solids* 227–230 (1998) 579.
- [21] J. Robertson, *Phys. Rev. B* 53 (1996) 16302.
- [22] R.A. Street, *Adv. Phys.* 30 (1979) 593.
- [23] R.A. Street, *Hydrogenated Amorphous Silicon*, Cambridge University Press, Cambridge, 1991.
- [24] B.A. Wilson, in: D. Adler and H. Fritzsche (Eds.), *Tetrahedrally Bonded Amorphous Semiconductors*, 1985 p. 397.
- [25] C. Godet, T. Heitz, J.E. Bourée, B. Drévilon, C. Clerc, *J. Appl. Phys.* 84 (1998) 3919.